Valorizing apple by-products as emulsion stabilizers: Experimental design for modeling the structure-texture relationships

Delphine Huc-Mathis, A. Guilbaud, N. Fayolle, V. Bosc, David Blumenthal

HAL Id: hal-02921437

https://agroparistech.hal.science/hal-02921437

Submitted on 3 May 2022

Valorizing apple by-products as emulsion stabilizers: experimental design for modeling the structure-texture relationships

D. Huc-Mathis[a], A. Guilbaud[a], N. Fayolle[b], V. Bosc[a] & D. Blumenthal[a]

[a] Université Paris-Saclay, INRAE, AgroParisTech, UMR SayFood, 91300, Massy, France
[b] JRS, Les Tanneries Royales, 20 quater rue Schnapper, 78100 Saint Germain en Laye, France

Key words

Vegetal particles; Pickering emulsions; predictive modeling; stability; rheology; scale-up

Highlights

- Minimal-processed apple powder can stabilize a wide range of emulsions over 2 months.

- The powder amount drives the oil droplet diameter (linear relationship $1/D = f(m_p)$).

- The oil content and addition of biosourced polymer drive the emulsion rheology.

- Predictive models are obtained for droplet size, gel strength and viscosity.

- Proof of concept is obtained for scaling-up from 200 mL to 12 L.

Abstract

Apple pomace was tested for its stabilizing properties of emulsions, among 15 formulas organized as an experimental design with 4 factors: oil content, powder content, polymer content and time. A wide range of texture (viscosity at $10s^{-1}$ from 200 to 7,500 mPa.s) and oil droplet size (from 18 to 46 μm) was achieved. This strategy enlightened that oil, and in a lesser extent, polymer content, mainly drove the texture of the emulsions. The polymer content was the most significant parameter influencing the shear-thinning behavior of the emulsions (– 0.247). The amount of powder displayed a strong and significant negative impact on the oil droplet diameter (-1.007). A linear trend was even obtained between 1/droplet diameter and the powder amount. A good stability was achieved for 12 formula

1

among the 15, with no coalescence nor drainage obtained in the emulsions, even when submitted to accelerated aging. A scale-up was even possible from a lab 200 mL version of emulsion to a semi pilot version of 12 L. This study thus revealed the ability of some food by-products to be valorized as sole emulsion stabilizer, without any chemical modification, extraction, purification of fractionation, ensuring a virtuous circle.

1. Introduction

Pickering emulsions, *i.e.* stabilized by solid particles, discovered in the early 1900s by Ramsden followed by Pickering, have been attracting more and more interest in the past years, as alternatives to surfactants for stabilizing dispersed systems such as food, cosmetic and other bioproducts. In their review paper, Rayner et al. (2014) showed an exponential increase during the past decade in the number of both publications and patents with the key words "Pickering emulsion" or "particle stabilized emulsion". Among these studies, a specific focus was recently brought on biosourced particles as stabilizing agents, such as starch, cellulose, proteins, chitosan and other biopolymer-based particles (Rayner et al., 2014; Tavernier et al., 2016; Yang et al., 2017). Indeed, when aiming for biocompatibility and biodegradability, inorganic particles such as latex, silica, mica etc, which were studied a lot (Yang et al., 2017; Aveyard et al., 2003), cannot be considered anymore. Moreover, apart from surfactant reduction or replacement, Pickering particles stabilization is expected to bring a very good stability against coalescence, should be able to resist well to varied physicochemical conditions such as pH, temperature, ionic strength etc, which may result in new mouthfeel and/or topical perceptions.

However, among the authors studying biobased particles for food- or topical-edible emulsions, the major part of the studies still relies on chemically modified particles, such as OSA starch (Li et al., 2019; Marto et al., 2015; Marku et al., 2012; Sjoo et al., 2015; Song et al., 2015; Timgren et al., 2011; Yusoff&Murray, 2011). While this strategy worked well with silica, clay and other inorganic particles, one could wonder its consistency with biosourced, biocompatible and biodegradable components. Therefore, other authors focused on natural particles, evaluating their potential as stabilizers, which can bring some new added value: cellulose particles (Jia et al., 2015; Tamayo Tenorio et al., 2017;

2

Wallecan et al., 2015), native starch from different botanical sources (Li et al., 2013) cocoa particles (Gould et al., 2013 Joseph et al., 2018), fat particles (Rousseau, 2013; Schröder et al., 2019), and proteins (Ren et al., 2019). Among these studies, few particles were retrieved only from thermomechanical processes such as grinding, milling, drying etc, while the majority required adding some more steps (delipidation, solvent extraction, purification, etc) in order to retrieve a fraction of interest.

Moreover, it can also be noted that the results available in literature were run on very small volumes of emulsion, ranging from 1 to 20 mL, except for Song et al. (2015) for example. Finally, experiments are rarely organized in order to take into account proper estimation of double interaction between the studied factors (formulation and/or process), while a strategy relying on experimental design could not only bring proper quantification of interaction, but also predictive modeling of several interesting indicators, such as texture and stability.

The aim of the present study was to evaluate how Pickering emulsions can be made from natural particles obtained from a food by-product (apple pomace), without using any fractionation, solvent or chemical modification. Our main hypothesis was that the insoluble content of apple pomace could act as an emulsion stabilizer, based on some previous experiments that needed to be formalized (Huc-Mathis et al. 2019). As a consequence, an experimental design was carried out in order to model several functional indicators of the emulsions, such as viscosity, shear-thinning behavior, gel strength and oil droplet diameter. 16 samples were analyzed, among which 15 formula and 1 repetition for the central point, allowing testing 4 factors: oil content (from 30 to 50%), apple powder quantity (70 – 110 mg/g of oil), biosourced polymer quantity (0.6 – 1.8%) and storage time at ambient temperature (Day0, Day35 and Day60). The addition of the biopolymer was tested in order to determine if Pickering emulsions already obtained in a proof of concept (Huc-Mathis et al., 2019) could be compatible with biopolymers, as regards to competition for water and depletion for example. Moreover, testing this mix was also interesting in order to modulate the amount of powder (thus solid particles) by modifying the bulk rheology through the polymer addition. Finally, 4 formulas were selected based on the obtained product map in order to be tested in accelerated aging conditions

3

(centrifugation or a one-month storage at 40°C). A first step towards scale-up was also tested, by making 12 L of one of the most promising formula at semi-pilot scale.

2. Materials & Methods

2.1 Characterization of the raw materials

The ultra-fine apple powder (VITACEL® CS 5), myritol 318 (0.948 g.cm^{-3} at 20 °C, 23 mPa.s at 20 °C) and the MCC polymer co-processed with xanthan gum (VIVAPUR® CS 032 XV) were kindly provided by JRS Retteinmaier (Rosengerd, Germany). Some potassium sorbate was added to all products through the aqueous phase with a 2.6 g.L^{-1} concentration. Apple powder was purposely chosen as a non-modified material, obtained after drying and micronizing a food byproduct (*Pyrus Malus* apple pomace), without using any solvent or additional step for extraction or purification. The physicochemical characteristics of the powder are the following: water content of 5% wt/wt, insoluble content of 90.5% wt/wt on dry matter and pectin content of 9% wt/wt on dry matter (from technical data sheet). The particle size of the dry powder was 5.3 ± 0.4 µm and its pH when hydrated in distilled water reached 4.50 ± 0.04.

The dry matter content was measured by placing 2 g of the powder in an oven at 105°C during 7h. The insoluble content was obtained as the difference between this total dry matter content and the dry matter content of the supernatant obtained after centrifuging 100 mL of powder dispersion (10% wt/wt into water + distilled water with potassium sorbate) at 10,000 rpm during 30 minutes at ambient temperature. For each measurement, a triplicate was carried out.

2.2 Experimental design & statistical analysis

The experiments were organized through a three-factor Central Composite Design (CCD). The axial value α was set at 1.682 in order to ensure the design rotability: the prediction variance depends only on the scaled distance from the center of the design. The randomized experimental design required 16 samples, among which a twice-repeated central point (Table 1). The 3 independent factors were the following: fat content (FC), from 30 to 50%wt; powder amount (Particle), from 70 to 110 mg.g^{-1} of oil

4

and the polymer amount (Polymer), from 0.6 to 1.8%wt. This design of experiments was used at 3 storage times, conducting at 3 series of measures (0, 35 and 60 days). The time was included as a forth independent factor.

Randomized CCD			ID	Oil Content (FC, %wt)	Powder content (Particle, mg.g^{-1} of oil)	Polymer content (Polymer, %)
0	0	- α	E898	40	56.7	1.2
1	1	-1	E465	50	70	1.8
0	- α	0	E963	40	90	0.2
-1	1	-1	E610	30	70	1.8
-1	-1	-1	E529	30	70	0.6
1	-1	-1	E733	50	70	0.6
1	1	1	E200	50	110	1.8
0	0	0	E415	40	90	1.2
0	0	0	E356	40	90	1.2
α	0	0	E149	56.8	90	1.2
-1	1	1	E926	30	110	1.8
-1	-1	1	E172	30	110	0.6
0	α	0	E781	40	90	2.2
1	-1	1	E378	50	110	0.6
0	0	α	E139	40	123.6	1.2
- α	0	0	E48	23.2	90	1.2

Table 1: Experimental design of the 16 studied emulsions - randomized central composite design with $\alpha = 1.682$

Data were analyzed based on JMP 14.1 software (SAS, Cary, North Carolina, USA). An effect was considered as significant if the corresponding P-value was lower than 0.05 (trust interval 95%). Finally, the postulated quadratic model was the following:

$$\forall i \in [1; 16], Y_i = \theta_0 + \theta_1 FC_i + \theta_2 Particules_i + \theta_3 Polymer_i + \theta_4 Time_i + \theta_5 FC_i^2$$

$$+ \theta_6 Particule_i^2 + \theta_7 Polymer_i^2 + \theta_8 Time_i^2$$

$$+ \theta_{12} FC_i.Particules_i + \theta_{13} FC_i.Polymer_i + \theta_{14} FC_i.Time_i$$

$$+ \theta_{23} Particules_i.Polymer_i + \theta_{24} Particules_i.Time_i + \theta_{34} Polymer_i.Time_i$$

$$+ \varepsilon_i \qquad with\ \varepsilon_i \xrightarrow{iid} N(0, \sigma^2)$$

There are as many models as measured variables to model Y.

Statistical analyses were performed with XLSTAT software (Addinsoft, France) and JMP® 14.1 software (SAS, Cary, North Carolina, USA.

2.3 Dispersion and emulsification processes

The lab protocol was taken from Huc-Mathis et al. (2019). Apple powder was dispersed in the oil phase using a Polytron rotor-stator (PTG 30/2, Kinematica AG, Switzerland) at 10,000 rpm during 2 min at ambient temperature. The water with potassium sorbate and the desired amount of polymer previously dispersed under 750 rpm agitation with magnetic bar during 20 min was added to the dispersion and the emulsification was carried out using the same device at 10,000 rpm during 3 min and placing the mixes in a cold bath in order to prevent any temperature increase during emulsification.

One emulsion (E139) was not only carried out at lab-scale but also using a semi-pilot protocol, with a colloidal mill (PROCESS-PILOT 2000/4, IKA, Germany) equipped with a 1 mm gap. Beforehand, the aqueous phase was made by mixing distilled water with the biopolymer using a deflocculating pale at 800 rpm during 20 min at ambient temperature. The same mixing protocol was applied to the oil phase, by mixing myritol 318 with apple powder. The latter phase was then set in the colloidal mill and the dispersion of the powder was completed by mixing during 7 min at 3170 rpm at 15°C. The two phases were then emulsified during 20 min at 4121 rpm at 20°C. 12 L of emulsion were retrieved from this scale-up trial. No temperature increase was evidenced in the emulsion during this scale-up.

2.4 Rheological measurements

Apparent viscosity (η, Pa.s), storage and loss moduli (G', Pa; G'', Pa) of the emulsions were measured using a MCR 301 rheometer (Anton Paar, Graz, Austria) with a striated plate- plate geometry (5 cm diameter, gap of 1 mm, using a solvent trap to avoid any change in water content). The temperature was set at 25 °C and controlled with a Peltier plate. All measurements were made in triplicate.

For flow measurements, the shear rate was set from 10 s^{-1} to 100 s^{-1}. Experimental data were fitted by a power law equation giving the shear-thinning index (n, -).

6

For dynamic measurements, a frequency sweep was carried out from 100 to 0.1 Hz, with a 0.2% strain, taken from the viscoelastic linear domain of all samples.

2.5 Particle size measurements

Particle size distribution was measured using a Mastersizer 2000 analyzer (Malvern Instruments, Worcestershire, UK). Measurements were carried out in a liquid cell at ambient temperature (RI = 1.545, RI dispersant = 1.33, Ab 0.1) on 10-fold diluted emulsions (with distilled water). Particle size distribution is expressed as volume of particles (%) = f(size (μm)). The average peak value was obtained out of the three repetitions were performed for each sample, at each day of measurement. Since the size distributions were not monomodal, as previously shown by Huc-Mathis et al. (2019), we chose the value of the peak attributed to the droplets (not the smallest one attributed to free particles).

2.6 Light microscopy

Dispersions and emulsions were observed under a light microscope (MZ6, Leica, Germany). Five snapshots per sample were taken at 10-, 20- and if necessary 50- fold magnification.

2.7 Emulsion stability with time

Two protocols for testing accelerated aging were applied for 4 selected samples: 1) storage of 30 mL samples in an oven set at 40°C, over 1 month, with one control placed at ambient temperature and a second control placed in the fridge at 4°C; 2) centrifugation at 3,000 rpm during 30 min at room temperature in 50 mL falcon tubes filled with 30 mL of emulsion.

3. Results & Discussion

3.1 Product mapping

The first challenge of a wide product space was to reach various textures, without deteriorating the stability towards coalescence, *i.e.* droplet diameter stability. All emulsions were found very shear-thinning with a shear-thinning index lower than 0.5 for all formulas. Then, Figure 1 represents the

evaluation of elastic modulus G', viscosity at 10 s⁻¹ and oil droplet diameter of the 16 emulsions with
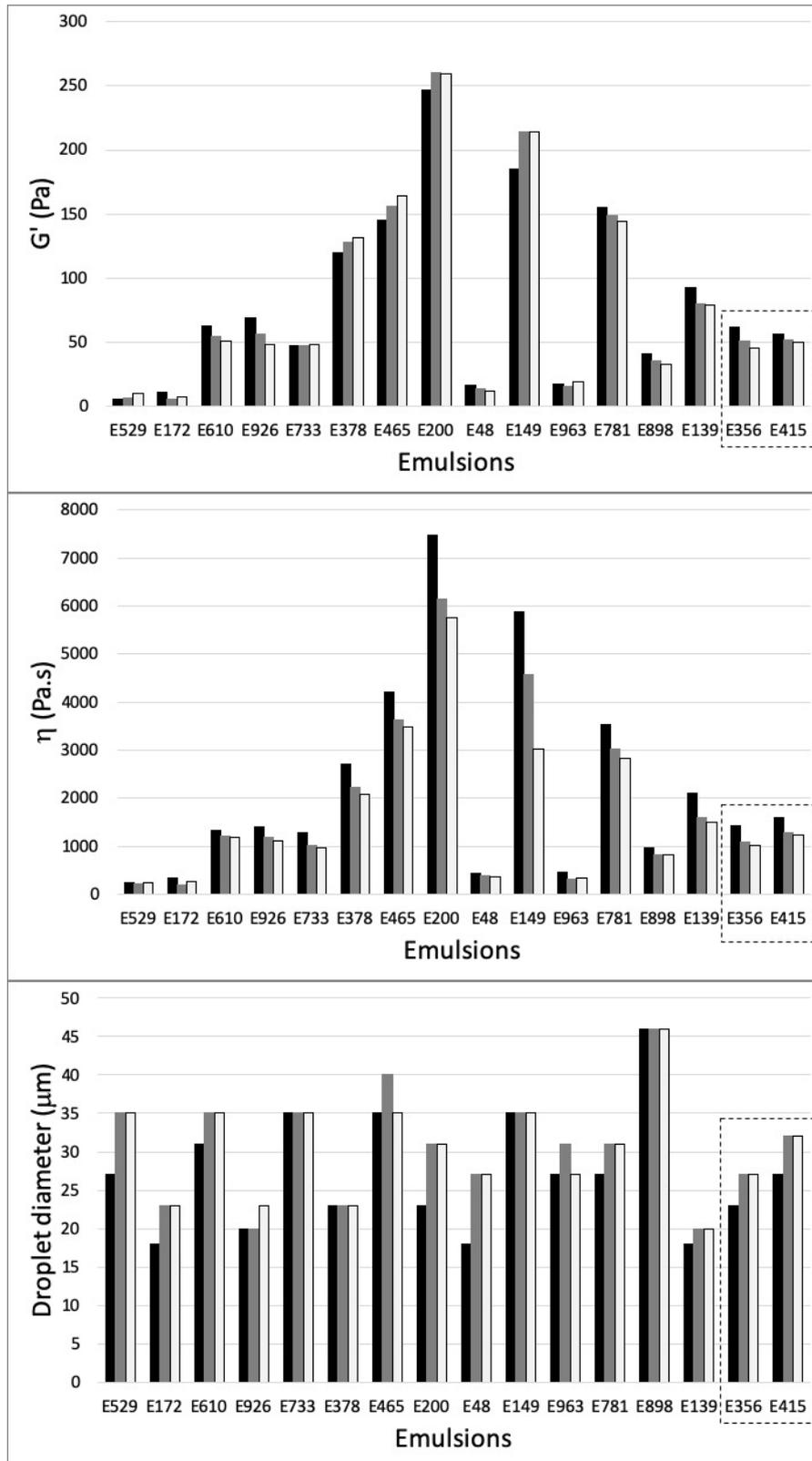
storage time.

Figure 1: Evolution with time (Day 0 in black, Day 35 in grey and Day 60 in white) of a) elastic modulus G', b) viscosity at 10 s⁻¹ η and c) oil droplet diameter. The coefficients of variation at Day0 are the following: from 1 to 11% for η (10 s⁻¹), 1 to 15% for G' (exception for E529 with 30%), 0 to 9% for oil droplet diameter.

A wide range of structure/texture properties was reached thanks to the experimental design: at Day 0, viscosity at 10 s^{-1} covered from 200 to 7,500 mPa.s, oil droplet diameter from 18 to 46 μm and G' from 5 to 250 Pa. For each indicator, the two samples of the central point (E356/E415) were close, as can be seen through the dotted lines circling on Figure 1. It allowed the calculation of their respective variations for viscosity, droplet diameter and G': 8%; 11%; 7% (values taken at Day 0). With time, the viscosity decreased and the elastic modulus increased or decreased. However, if the decrease of the viscosity with time can be considered significant regarding the duplicated formula, the variations of G' are always less or equal to the difference between the two repetitions of the central point. The droplet diameter could also slightly increase with time, even if it remained quite stable for most emulsions, especially between Day 35 and Day 60. The effect of storage time on structure/texture indicators is described afterwards thanks to the experimental design results and modeling. This was one of our main objective by using such strategy, not only to rely on observations, but to properly quantify significant effects and interaction. Only three samples displayed a variation higher than the one registered for the duplicated formula: E529, E200 and E48. However, it only occured between Day 0 and Day 35, since between Day 35 and Day 60, the diameter remained constant for these emulsions too. This would be consistent with some coalescence and/or aggregation occurring when there is not enough particles nor oil and/or when this cannot be compensated by the presence of a thickening agent in the continuous phase. Stating a very stable droplet diameter over two months, among the product space, is a very important result supporting the main hypothesis we made from the beginning: the powder shall stabilize the emulsions thanks to their solid particles. Indeed, such limited or avoided coalescence is a well described feature of Pickering emulsions. This shall be analyzed further based on the following results, in order to better understand the correlations, therefore the main impact of the different formulation parameters, on the functional properties of the final emulsions. Finally, the stability assessment was confirmed by performing not only size distribution measurements, but also light microscopy in order to have a direct look at the microstructure (Figure 2). Day 0 and Day 35 were chosen in order to illustrate these results over time, since they are the one where the maximal differences could be registered regarding the measurements of oil droplet diameter.
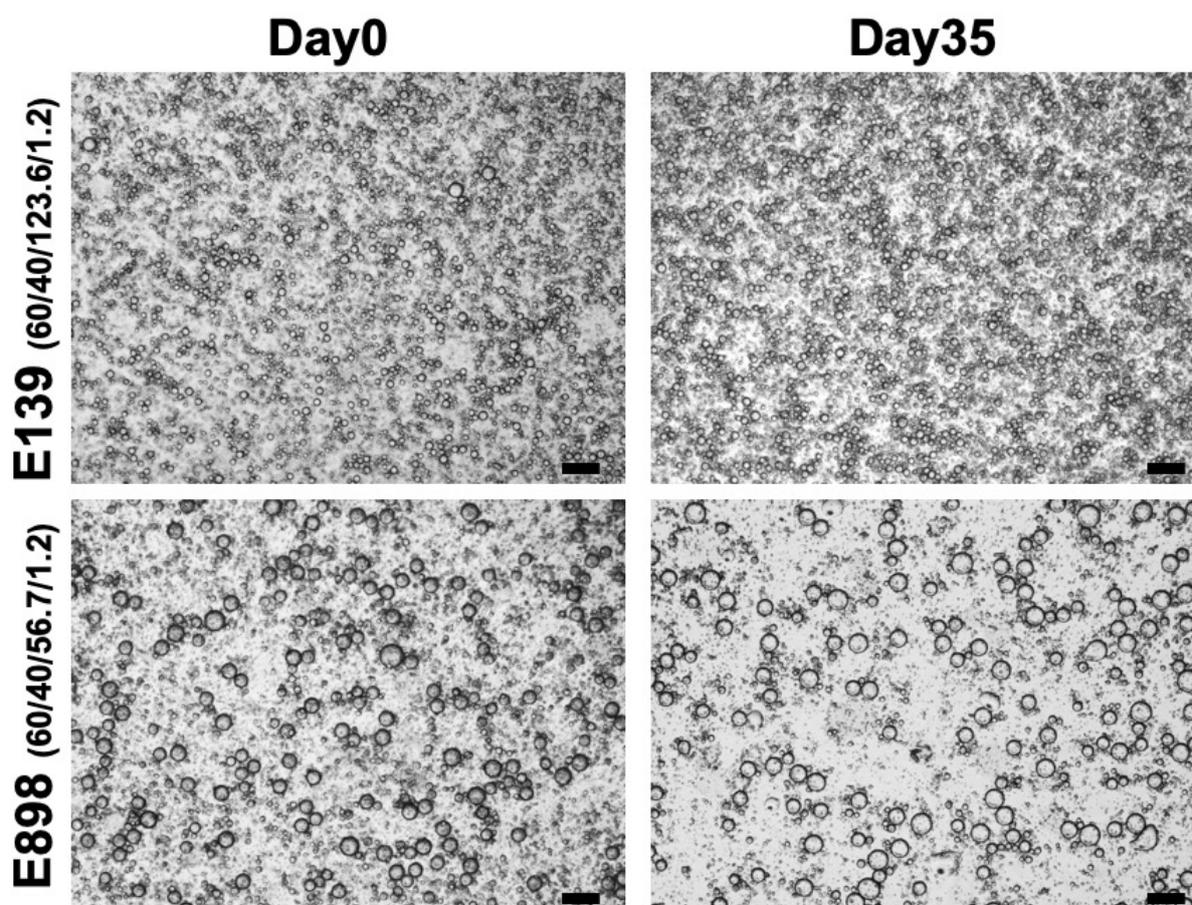
9

Figure 2: Light microscopy for emulsion E139 and E898 diluted 1/3 (in lines) at Day0 and Day35 (in columns). Codes for emulsions: water content(%)/oil content(%)/powder quantity(mg.g^{-1} of oil)/polymer content(%). Magnification x10, scale bar = 100 μm

The micrographs showed consistent results with Figure 1c, since it could be observed that for the two emulsions taken as examples (in the objective of covering a wide range of droplet size inside the product space), the droplet size was indeed the lowest for E139 and the highest for E898. For both of them, it was impossible to differentiate the emulsions based on their microstructure from Day0 and Day35. Finally, regarding visual stability it has to be noted that among the 15 formulas, 2 were submitted to a small draining during the 2 months-storage at room temperature, with a ratio between the drained phase height over the total product height of 10.4% for E963 and 12.5% for E529.

The 16 emulsions were then mapped through PCA in order to determine how well the products were discriminated and according to which main indicators. They could also be related to the three

formulation factors tested in the experimental design (oil content, polymer content and powder content), as can be seen in Figure 3.
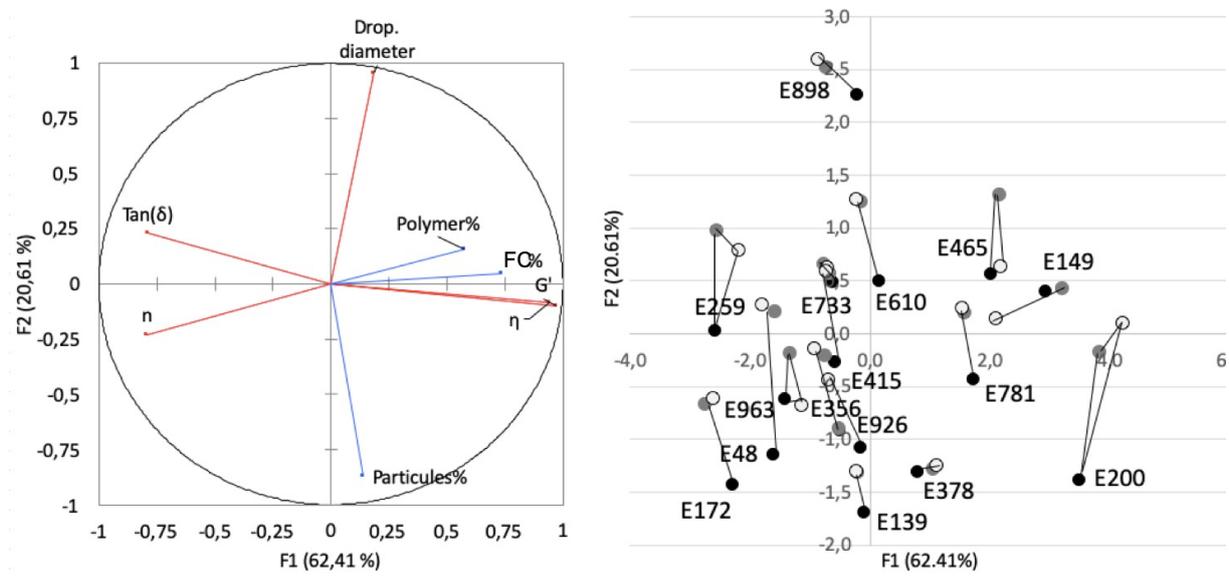

Figure 3: a) Correlation circle with constitutive variables in red and supplementary variables in blue; b) PCA map on (F1; F2) for the 16 products monitored from D0 (black) to D35 (grey) and D60 (white) so as the different times are linked together by black lines.

The first observation is that the product space is well-covered by the different samples, and 83% of the overall information can be displayed on the two main axes (F1; F2), *i.e.* rheology and droplet size, as can be seen on the correlation circle (Figure 3a). Secondly, it should be noted that for some products, Day0, Day35 and Day60 were almost superimposed, such as E378, E139 and E733, or closed, such as E963, E898, E465, E149, E781, E356, E926, E172, E259, E415 and E733. There is more difference over time for E200 and E48 since Day0, Day35 and Day60 are further away on the map. Moreover, when a distance is created in time, it is always along F2, which is driven by the oil droplets diameter, except for E149. However, looking at the variation between the two samples of the repeated formula (central point of the experimental design E415 and E356), it can be deduced that: i) the two samples are close to each other, especially regarding rheology (F1 axis) and ii) the distance between the three days gives a trust interval that is higher or equal to all other distances except for E200 and E48. The latter might therefore be considered as more variable than the other formula. As can be seen on Figure 1, the reproducibility of the repeated formula is good (variation of 8% for viscosity and 11% for droplet diameter for example). Finally, the 3 formulation factors of the experimental design (oil content, polymer content and particles charge) were added as supplementary data on the PCA map.

11

The oil content was significantly represented on F1; the powder quantity on F2 and the polymer content on F3. The powder quantity is therefore the main factor driving the oil droplet size, since it is significantly anticorrelated to the droplet diameter (-0.84 according to the Pearson correlation matrix). Such a strong correlation coefficient shows that the powders, especially their solid particles, are the key stabilizing elements, supporting the first hypothesis that the present emulsions were indeed stabilized by the by-product powders, as expected from the proof of concept enlightened by Huc-Mathis et al. (2019). One could wonder if the added biopolymer could participate to the coalescence limitation, however no correlation could be evidenced between added polymer and particle size. On the contrary, the powder displayed no effect on the rheological properties when the biopolymer is added. Therefore, the modelling strategy allowed a finer understanding of the main roles of different ingredients, classically used in realistic conditions of emulsions' formulation. Then, the oil content was also significantly correlated with the droplet diameter, but with a much lesser Pearson coefficient (0.31). It will be interesting to look at the double interaction between powder quantity and fat content within the CCD analysis. The oil content is the one factor significantly correlated to all variables, rheology, diameter and backscattered light all together, with the highest Pearson coefficient with tan(δ) and G'. As for the polymer content, it is significantly correlated to the shear-thinning index with a Pearson coefficient of -0.86, and in a lesser extend with the viscosity and G' (0.52 for both correlation).

The direct correlation between the powder content as regards to oil content (mg of powder.g^{-1} of oil) and the oil droplet diameter can be observed over time, from Day0 to Day60, as can be seen on Figure 4.
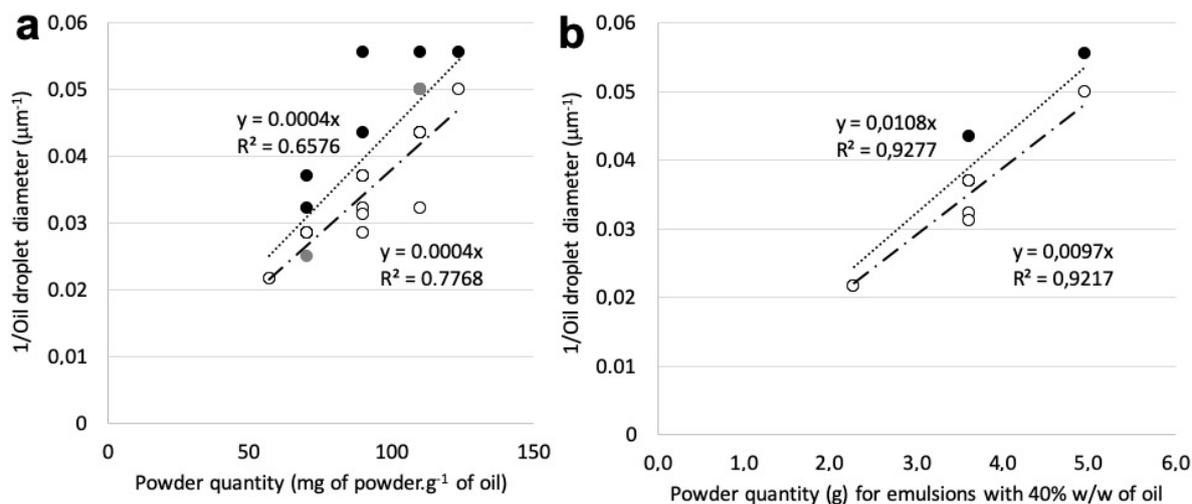
Figure 4: Evolution of 1/Oil droplet diameter with a) the amount of apple powder for all emulsions and b) for emulsions containing 40% of oil, for the 3 days (Day0 in black, Day35 in grey and Day60 in white). All points are displayed even if there are some superimpositions in b).

The relationship between the oil droplet diameter and the amount of powder was very straightforward based on the previous product mapping. However, the so-called "amount of powder" is in fact a mass of powder per gram of oil. This nomenclature is very common in solid particles-stabilized emulsions. Keeping that in mind, the 1/diameter = f(powder amount) global curves could be fitted by linear trends, with $R^2 = 0.66$ at Day0 and $R^2 = 0.78$ at Day60, as can be seen on Figure 4a. When isolating one population of emulsions based on one fraction of oil, for example 40% w/w, the relationship is becoming even clearer (Figure 4b). Linear trends are perfectly fitting, with $R^2 = 0.93$ at Day0 and $R^2 = 0.92$ at Day60 (the 4 points are displayed for both times but some of them are hidden due to superimposition). It worked as well for 30% and 50% of oil too, but only two masses of powder were tested for these emulsions (70 and 110 mg.g^{-1} of oil), making it less interesting to fit a linear trend. This proportionality is strong evidence that the underlying mechanism for oil droplet stabilization is indeed occurring through solid particles anchoring at the oil/water interface, *i.e.* Pickering emulsion, even though the created interface is probably hybrid, with soluble components adsorbed as well. It helps to better understanding the results obtained in a previous work (Huc et al., 2019), where we showed a proof of concept for emulsions solely stabilized by apple powder, but without being able to decorrelate between the role of the insoluble particles at the interface and their role in the continuous phase (creation of a gel-type network). Here, it is clear that the powder quantity is directly driving the

13

oil droplet diameter for a given oil volume and a given energy (homogenization is always the same). This linear relationship between the droplet diameter and the particle amount was assessed many times in literature for inorganic particles, such as latex, silica or carbon tubes (Arditty et al., 2003; de Folter et al., 2013; Joseph et al., 2018; Wang & Hobbie, 2003; Wu et al., 2015). The authors recalled that the asymptotic limit of the surface coverage at infinite time s_f ($m^2.g^{-1}$) can be determine when knowing the volume of oil, the slope of the experimental curve giving $1/D = f(m_p)$ where m_p is the mass of particles and D the oil droplet diameter, and assuming that the degree of surface coverage is $\tau \rightarrow 1$ (total and irreversible anchoring of particles at the interface). It our case, taking 40% w/w of oil as the reference emulsions, knowing the density of myritol oil (0.948 $g.cm^{-3}$) and the slope 9.724 $m^{-1}.g^{-1}$ of the $1/D = (m_p)$ curve at Day 60, it can be calculated that $s_f = 2.2$ $m^2.g^{-1}$. This is consistent with Arditty et al. (2003) who found $s_f = 3.1$ $m^2.g^{-1}$ for o/w emulsions stabilized by silica particles partially hydrophobized by a graft of n- octyltriethoxysilane on their surface (from 0.1 to 1 µm for the particle size). It was lower than the limit surface coverage found by Joseph et al. (2018) for o/w emulsions stabilized by delipidated cocoa particles ($s_f = 17$ $m^2.g^{-1}$). Therefore, the anchoring of particles at the interface is meant to depend not only on the particle size, but also on other properties, such as morphology, surface charge, etc.

3.2 Experimental design: modelling emulsion functionalities

Based on the previous measured variables (Y) defined as droplet diameter D, viscosity η, elastic modulus G', ratio between viscous and elastic moduli tan(δ) and shear-thinning index n, the statistical analysis of the response surface design could be carried out based on 4 factors: fat content (FC), particles content (Particles), polymer content (Polymer) and time (Time). We obtained five models, one for each Y. Regression coefficients were calculated for each model and an analysis of variance (ANOVA) was performed for the evaluation of the model performance (F test for significance and coefficient of determination R^2).

The p-value of each factor corresponded to the lowest p-value of the effect amongst all models for the response variables and was expressed as a LogWorth value (LogWorth = $-log_{10}$(p-value)). This index allowed us to simplify the models. We took into account all the measured variables at once: the most

14

significant effects ($p \leq 0.05$) were selected from the ranking using a backward elimination procedure. The coefficients of the simplified models are displayed in Table 2.

	Droplet diameter	G'	Tan(δ)	Viscosity (10s-1)	n	Multi objective selection of effects
F Ratio	F(12,35)=27.0	F(12,35)=381.2	F(12,35)=23.2	F(12,35)=85.4	F(12,35)=26.9	
Prob > F	≤0.0001	≤0.0001	≤0.0001	≤0.0001	≤0.0001	
R²	0.90	0.99	0.88	0.97	0.90	

Terms	Coefficients					LogWorth
Constante	83.252***	680.892***	0.438	16 182.266***	0.185	
FC	-0.095	-24.756***	0.000	-554.002***	0.014**	18.76
FC*FC	0.001	0.207***	0.000	4.642***	0.000**	15.90
FC*Particules	0.002	0.110***	0.000	2.445***	0.000**	15.77
FC*Polymer	0.125	2.883***	0.003**	100.396***	0.002*	12.70
FC*Time	-0.003	0.016**	0.000*	-0.924***	0.000	3.42
Particules	-1.007***	-5.165***	0.001	-121.320**	0.004	7.64
Particules*Particules	0.003*	0.008*	0.000	0.143	0.000	1.81
Particules*Polymer	0.021	0.240	0.001	14.607*	0.001	1.58
Polymer	-5.284	-146.162***	-0.059	-5 173.762***	-0.247***	8.88
Polymer*Polymer	-0.139	32.286***	-0.069***	619.937**	0.003	8.94
Time	0.307**	-0.672**	0.003*	22.623	0.000	2.93
Time*Time	-0.002*	0.000	0.000	0.081	0.000	1.41
Polymer x Time	Out of the models					
Particles x Time	Out of the models					

Table 2: Impact of significant variables: fat content (FC), particles amount (Particles), polymer content (Polymer) and time (Time) on the models using response surface design (data were considered significant if P-value ≤ 0.05).

The individual impact of the 4 factors on each Y was evaluated in order to estimate the significant ones, including 2nd order interactions. All variables and interactions are significant for at least one of the five models, except for Polymer x Time and Particles x Time. The most impacting factor seems to be the fat content, followed by particles and polymer contents, then time. It can also be seen that the multi objective selection of factors implies to keep some effects or interactions even if they are significant for only one or two measured variables: it is the only way to have the same base for the response surfaces for all the measured variables.

Keeping in mind that the design of experiments was chosen in order to minimize the correlation between terms of the models, it is then possible to interpret the sign of the coefficients. Table 2 clearly shows how the 4 factors are influencing the different measured variables, characterizing the emulsions.

15

For example, the oil droplet diameter is only significantly impacted by the particles content and time, both in a quadratic way. The negative coefficient for particles shows that the more powder used in the formulation, the lesser droplet diameter will be obtained in the resulting emulsion. There again, the direct link between powder amount and the droplet size, i.e. stability against coalescence or aggregation, appeared very straightforward. On the contrary, time displayed a positive impact on the droplet diameter, meaning that the droplet size is slightly increasing with time, while $time^2$ has a negative impact on the droplet size. One could wonder if in such conditions, time is really a proper lever for droplet diameter evolution, especially since the coefficients (0.3 for time and – 0.002 for $time^2$) are much smaller than the coefficient of particle content (-1,007). This is comforting the fact that particles content is the most important factor driving the droplet size in the emulsions, as previously hypothesized on the linear relationships displayed on Figure 4.

Finally, the profiles of the measured variables Y could be plotted as a function of the 4 variables X1, X2, X3 and X4 (Figure 5), which can be used to predict each effect. It allowed us to optimize the results, defining target values for the variables and identifying the needed values for the variables.
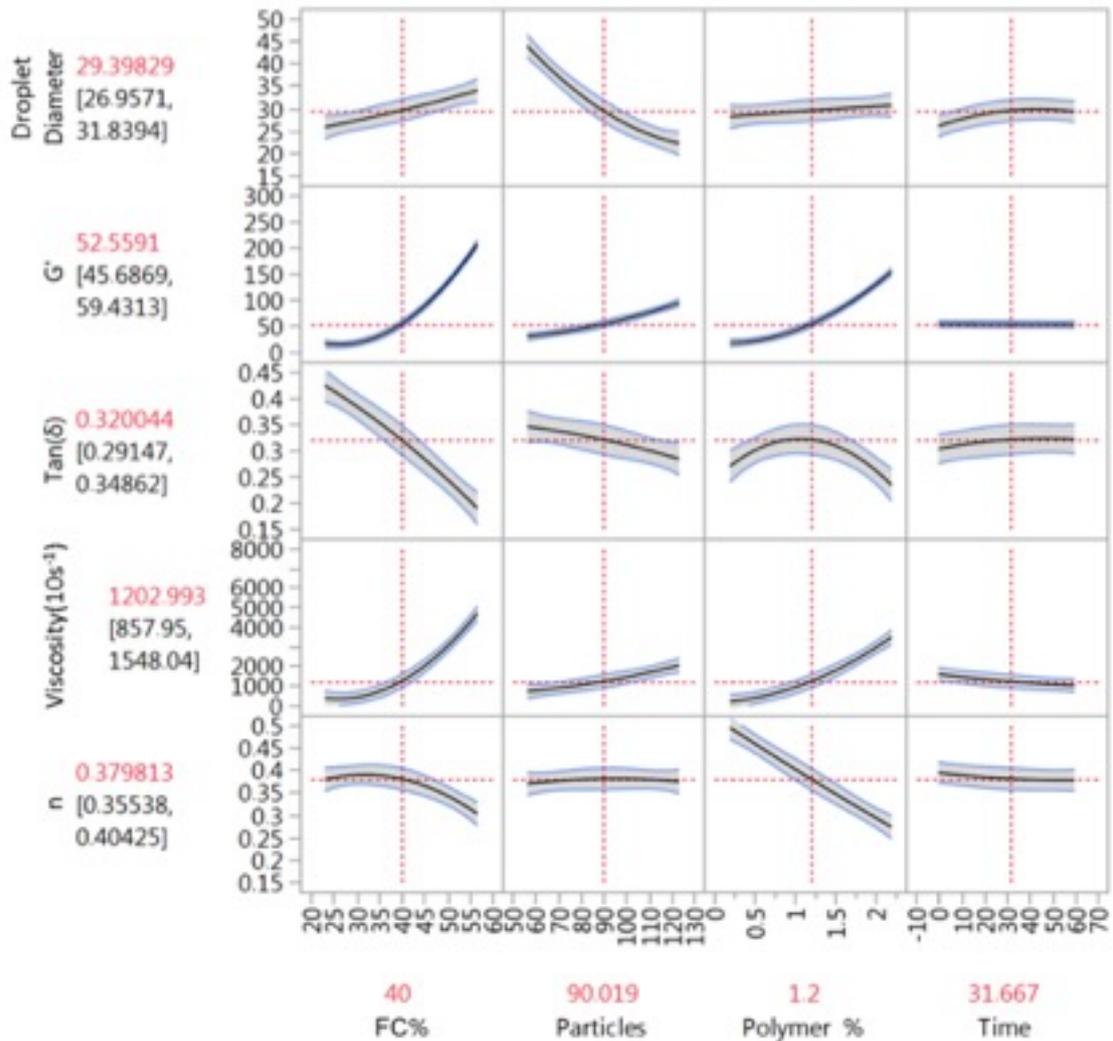
Figure 5: Profiles of Y = f(X) for the 4 tested variables: fat content (FC%, X1), powder content (Particles, X2), polymer content (Polymer%, X3) and time (Time, X4). The black line is the calculated model and the grey zone corresponds to the 95% confidence interval.

The five measured variables all appeared well predicted regarding how close the grey zone is to the calculated model (black line). Some effects were very strong, as for example: 1) the highest the powder content, the lowest the oil droplet diameter as previously explained from the study of the coefficients (first line); 2) the highest the fat and polymer contents, the highest the elastic modulus G' and the viscosity and the lowest tan(δ) (second, fourth and third lines); 3) the highest the polymer and fat contents, the lowest the shear thinning index n (fifth line). It can also be noted that time (last column, X4) displayed very little effect on the variables of droplet size, viscosity, tan(δ) and n and no effect at all on G', which was very satisfactory in order to reinforce the assertion of so called "stable" emulsions.

17

Therefore, using this experimental design approach and because of the orthogonality of the factors and their 2nd order interactions, we were firstly able to better understand the influence of the different variables on the structure and stability of the emulsions. It was also possible to obtain a statically significant hierarchy among them, and to model their effect on each measured variable, which are the most common indicators usually chosen for describing functional properties of emulsions, especially stability.

This is the final lock that remains to be overcome. Indeed, how to appreciate stability is something very difficult since this is a meta-descriptor, that can be approached by a combination of various measurements (such as the size of the dispersed elements, the rheological variables, the light/material interaction etc) which are multiscale and only relevant in a time-dependent perspective. The present work still allowed to assess the effect of time as a variable on its own, and to study its interactions with formulation variables.

3.3 Accelerated aging

The size distribution was monitored over a month at 40°C for four emulsions selected after product mapping: E610, E465, E139 and E898. This choice was based on the following criteria: E898, E610 and E139 displayed a close texture as can be seen by projecting their location on the PCA map on the main axis F1. However, they possessed very different oil droplet sizes. In the same way, E898, E610 and E465 displayed closed oil droplet sizes, as can be seen by projecting their location on the main axis F2 of the PCA map. However, they had quite different projections on F1, regarding texture properties. It thus seemed interesting to choose these 4 emulsions in order to cover a wide range of products on the PCA map and also to compare the results as regards to texture and oil droplet size, which are two of the most common indicators for characterizing emulsions. A control sample for each

one of them was placed in the fridge at 4°C and a second one was stored at ambient temperature

(repetition from the previous tests), so its size distribution could also be measured at Day35 as control.
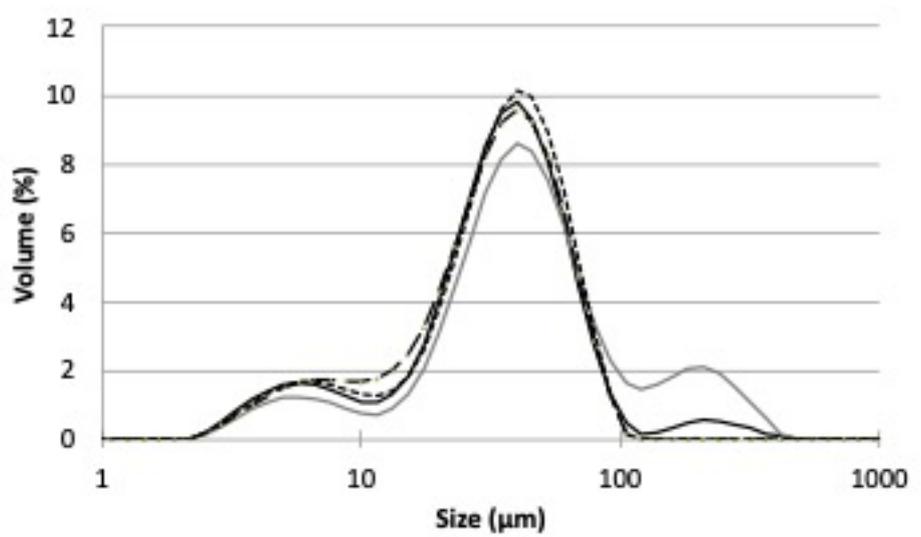

Figure 6: Size distribution of E898 over time during 1-month storage at 40°C. Day0 in continuous black line, Day7 in continuous grey line, Day35 in short dotted line and Day35 at 4°C in long dotted line.

The four emulsions followed during accelerated aging in the oven displayed a constant oil droplet

diameter over time, as can be seen for example for E898 from Day0 to Day35 at 40°C (Figure 6). The

four curves are very similar. Two or three peaks can be observed: #1 is attributed to the particles,

around 7 μm; #2 corresponds to the oil droplets and #3 when it exists can be attributed either to

coalescence/aggregation and/or to a clogged cell in the granulometer. Since Peak #3 was especially

visible at Day7 for all the samples, while at Day35 no sample displayed any sign of it, the latter

hypothesis shall be the right one. The sizes attributed to the oil droplets for the four emulsions were

the following: 20 μm for E139, 35 μm for E610 and E465 and 40 μm for E898. It can be noted that

these values are in good accordance with the previous data measured during the experimental plane,

confirming the ± 4 μm variation for the oil droplet size reproducibility. Therefore, no change could be

noted, either due to the 1-month storage at 40°C, or to the temperature, since at Day35, samples stored

at 4°C, ambient temperature and 40°C displayed the same size distributions.

This resistance to accelerated aging was confirmed by a second verification carried out by submitting

the four emulsions to centrifugation. Among the four samples, none of them displayed any kind of

creaming or draining. Only one (E898) displayed a slight decantation, as can be seen on Figure 7.

Figure 7: Small decantation after 30 min at 3,000 rpm for E898

This small decantation appeared whiter than the rest of the emulsion. It is difficult to attribute it to something else that the apple powder, even if it is overall brown. Maybe this is due to a specific fraction of the powder or to an excess of particles that would not be anchored at the oil/water interface, this is yet to be confirmed. Therefore, the four emulsions selected in order to cover the product space obtained in the present study well-resisted to accelerated aging performed under two different protocols.

3.4 Semi-pilot scale-up

The last step of the present work was to assess how transferable the lab-scale emulsions were. We performed a scale-up by making 12L of E139 at 4,121 rpm during 20 minutes at ambient temperature. We based this choice on the fact that E139 displayed the smallest oil droplet size at lab-scale. We wanted to check whether or not we would be able to reach it at semi-pilot scale, even though the shear rate, geometry, thus overall energy during emulsification, was meant to be different. Indeed, solid particles-stabilized emulsions are known to give bigger oil droplet size than classical emulsions. Therefore, we thought the scale-up trials would make more sense if we were able to reach a small oil droplet diameter, even though our 20 μm target is still bigger than the usual range of size for classical emulsions. The main characteristics of the obtained emulsion were compared with the corresponding

20

lab-scale sample made during the experimental design, as can be seen for example at Day7 for size distribution and flow curve on Figure 8. The emulsions were compared at Day7 due to logistic reasons, since no conservative agent was used for the pilot-scale process.
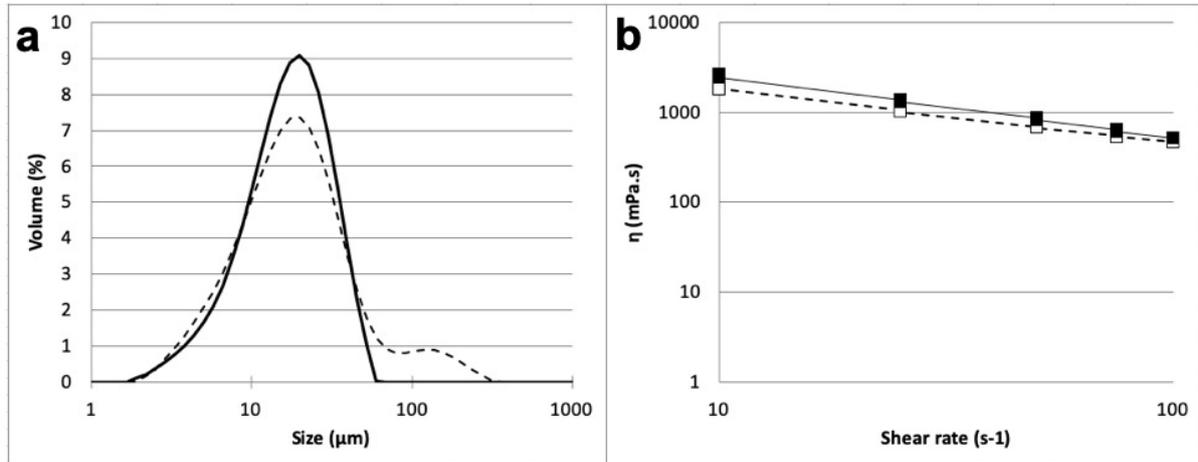

Figure 8: Comparison between lab-scale (dotted line or white) and pilot-scale (continuous line or black) versions of E139 at Day7 (60% water, 40% oil, 123.6 mg of powder.g^{-1} of oil, 1.2% of biopolymer).

The size distributions (Figure 8a) were very close except for a small peak at 140 µm displayed by the lab-scale E139 at Day7 (but it was absent again at Day35 and Day60). The oil droplets were considered as the main population and therefore displayed the same average diameter of 20 µm. The main peak still exhibits a trail towards small sizes which can be attributed to the particles themselves (around 6 µm).

The flow properties were also quite close between lab- and pilot-scale versions of E139 (Figure 8b). The shear-thinning index was 0.32 for pilot-scale E139 and 0.39 for lab-scale E139. The viscosity at 10 s^{-1} and 20°C reached 2.4 Pa.s for pilot-scale E139 against 1.7 Pa.s for lab-scale E139. Therefore, the present experiment also represents a good proof of concept of scaling-up some Pickering oil in water emulsions only made with apple byproduct powder as stabilizing agent and a biopolymer for adjusting the desired texture through the continuous phase.

4. Conclusion

The objective of the present study was to understand how a raw and minimal processed byproduct such as apple pomace powder could be used as stabilizer of oil in water emulsions. An experimental

21

design approach was chosen and 15 different formula were tested, giving a wide range of structures and textures in the obtained product space. A visual stability (no draining, sedimentation or creaming) was achieved for 12 of them, with oil content ranging from 30 to over 50%. A microscopic stability (oil droplet size) was also achieved for the major part of the formulas. These results are backing up the hypothesis of a solid particles-stabilized emulsions, which could be a Pickering mechanism and or the creation of a network in the continuous phase. This remains the final step of a study that could go further in the analysis of insoluble vs soluble components of the by-products, in order to prioritize these two leads. The interest of the insoluble particles is still one of the main outputs of the present study, where the experiments were designed in order to be as applicable as possible for formulation and innovation. We also successfully performed accelerated aging tests and a scale-up step from 200 mL to 12 L at a semi-pilot scale. As for the final models, they represent a ready-to-use toolbox quantifying the effects of oil (myritol 318), powder (apple pomace as a whole, without any fractionation) and biopolymer (MCC co-processed with xanthan) contents, as well as giving a quantification of the time effect. Double interactions were checked and the models can be adjusted in order to target desired properties of the final emulsions, such as specific texture (through viscosity and gel strength for example) and microstructure (with droplet diameter). This will give access to different products, especially since the present study also confirmed that the by-product apple powder is compatible with a biopolymer. Therefore, the relevance of this research could relate to various applications, in order to meet consumer's demands for more naturalness and clean label products. These could be food of course, such as sauces, or vegetal-based analogues for dairy products for example, since apple pomace shall represent some interest as stabilizer, but also thanks to its high fiber content. The present results would also fit very well other applications such as cosmetics and bioproducts. Our next challenge will be to determine whether or not some other food byproducts, still unpurified, unmodified and ideally as minimally processed as possible, could be as good candidates (as apple pomace powder is) for stabilizing emulsions, always in industry relevant conditions.

Acknowledgements

References

Arditty S., Whitby C.P., Binks B.P., Schmitt V., Leal-Calderon F. (2003). Some general features of limited coalescence in solid-stabilized emulsions. *The European Physical Journal*, 11: 273-281.

Aveyard R., Binks B.P., Clint J.H. (2003). Emulsions stabilised solely by colloidal particles. Advances in Colloid and Interface Science, 102-103: 503-546.

de Folter J.W.J., Hutter E.M., Castillo S.I.R., Klop K.E., Philipse A.E., Kegel W.K. (2014). Particle Shape Anisotropy in Pickering Emulsions: Cubes and Peanuts. *Langmuir*, 30: 955-964.

Gould J., Vieira J., Wolf B. (2013). Cocoa particles for food emulsion stabilization. *Food & Function*, 4: 1369-1375.

Huc-Mathis D., Journet C., Fayolle N., Bosc V. (2019). Emulsifying properties of food by-products: Valorizing apple pomace and oat bran. *Colloids and Surface A*, 568: 84-91.

Jia X., Xu R., Shen W., Xie M., Abid M., Jabbar S., Wang P., Zeng X., Wu T. (2015). Stabilizing oil-in-water emulsion with amorphous cellulose. *Food Hydrocolloids*, 43: 275-282.

Joseph C., Savoire R., Harscoat-Schiavo C., Pinton D., Monteil J., Leal-Calderon F., Faure C. (2018). O/W Pickering emulsions stabilized by cocoa powder: Role of the emulsification process and of composition parameters. *Food Research International*, 113: 755-766.

Li C., Li Y., Sun P., Yang C. (2013). Pickering emulsions stabilized by native starch granules. *Colloids and Surfaces A: Physicochemical and Engineering Aspects*, 431: 142-149.

Li S., Li C., Yang Y., He X., Zhang B., Fu,X., Ping Tan C., Huang Q. (2019) Starch granules as Pickering emulsifiers: Role of octenylsuccinylation and particle size. *Food Chemistry*, 283: 437-444.

Lu X., Zhang H., Li Y., Huang Q. (2018). Fabrication of milled cellulose particles-stabilized Pickering emulsions. *Food Hydrocolloids*, 77: 427-435.

23

Marto J., Gouveia L., Jorge I.M., Duarte A., Gonçalves L.M., Silva S.M.C., Antunes F., Pais A.A.C.C., Oliveira E., Almeida A.J.., Ribeiro H.M. (2015). Starch-based Pickering emulsions for topical drug delivery: A QbD approach. *Colloids and Surfaces B: Biointerfaces*, 135: 183-192.

Marku D. Whalgren M., Rayner M. Sjöön M, Timgren A. (2012). Characterization of starch Pickering emulsions for potential applications in topical formulations. *International Journal of Pharmaceutics*, 428: 1-7.

Rayner M., Sjöö M., Timgren A., Dejmek P.. (2012). Quinoa starch granules as stabilizing particles for production of Pickering emulsions. *Faraday Discussions*, 158: 139–55.

Ren Z., Chen Z., Zhang Y., Lin X., Li B. (2019). Novel food-grade Pickering emulsions stabilized by tea water-insoluble protein nanoparticles from tea residues. *Food Hydrocolloids*, 96: 322-330.

Rousseau D. (2013). Trends in structuring edible emulsions with Pickering fat crystals. *Current Opinion in Colloid & Interface Science,* 18(4): 283-291.

Schröder A., Sprakel J., Boerkamp W., Schröen K., Berton-Carabin C. (2019). Can we prevent lipid oxidation in emulsions by using fat-based Pickering particles? *Food Research International*, 120: 352-363.

Sjoo M., Cem Emek S., Hall T., Rayner M., Wahlgren M. (2015). Barrier properties of heat treated starch Pickering emulsions. *Journal of Colloid and Interface Science*, 450: 182-188.

Song X., Pei Y, Qiao M., Ma F., Ren H. (2015). Preparation and characterizations of Pickering emulsions stabilized by hydrophobic starch particles. *Food Hydrocolloids*, 45: 256-263.

Tamayo-Tenorio A., Gieteling J., Nikiforidis C.V., Boom R.M., van der Goot A.J. (2017). Interfacial properties of green leaf cellulosic particles. *Food Hydrocolloids*, 71: 8-16.

Tavernier I., Wijaya W., Van der Meeren P., Dewettinck K., Patel A.R. (2016). Food-grade particles for emulsion stabilization. *Trends in Food Science & Technology*, 50: 159-174.

Timgren A., Rayner M., Sjöö M., Dejmek P. (2011). Starch particles for food-based Pickering emulsions. *Procedia Food Science*, 1: 95–103.

Wallecan J., McCrae C., Debon S.J.J., Dong J., Mazoyer J. (2015). Emulsifying and stabilizing properties of functionalized orange pulp fibers. *Food Hydrocolloids*, 47: 115-123.

Wang H., Hobbie E. (2003). Amphiphobic Carbon Nanotubes as Macroemulsion Surfactants. *Langmuir*, 19(8) : 3091-3093.

Wiley R.M. (1954). Limited coalescence of oil droplets in coarse oil-in-water emulsions. *Journal of Colloid Science*, 9: 427-437.

Wu T., Wang H., Jing B., Liu F., Burns P.C., Na C. (2015). Multi-body coalescence in Pickering emulsions. *Nature communications,* 6:5929.

Yang Y., Fang Z., Chen X., Zhang W., Xie Y., Chen Y., Liu Z., Yuan W. (2017). An Overview of Pickering Emulsions: Solid-Particle Materials, Classification, Morphology, and Applications. *Frontiers in Pharmacology*, 8:287.

Yusoff A., Murray B. S. (2011). Modified starch granules as particle-stabilizers of oil-in-water emulsions. *Food Hydrocolloids*, 25(1), 42–55.